# Turkish Journal of Engineering

*Turkish Journal of Engineering (TUJE)*
*Vol. 4, Issue 1, pp. 36-46, January 2020*
*ISSN 2587-1366, Turkey*
*DOI: 10.31127/tuje.571598*
*Research Article*

## INVESTIGATION OF THE MOMENT–CURVATURE RELATIONSHIP FOR REINFORCED CONCRETE SQUARE COLUMNS

Saeid Foroughi *[1] and Süleyman Bahadır Yüksel [2]

[1] Konya Technical University, Faculty of Engineering and Natural Sciences, Department of Civil Engineering, Konya / Turkey
ORCID ID 0000-0002-7556-2118
saeid.foroughi@yahoo.com

[2] Konya Technical University, Faculty of Engineering and Natural Sciences, Department of Civil Engineering, Konya / Turkey
ORCID ID 0000-0002-4175-1156
sbyuksel@ktun.edu.tr

* Corresponding Author
Received: 29/05/2019 Accepted: 11/09/2019

**ABSTRACT**
In this study; the effect of the material model, axial load, longitudinal reinforcement ratio, transverse reinforcement ratio and transverse reinforcement spacing on the behavior of reinforced concrete cross-sections were investigated. Squared cross-section column models have been designed. The effect of axial load, transverse reinforcement diameter and transverse reinforcement spacing on the behavior of reinforced concrete column models have been analytically investigated. The behavior of the columns was evaluated from the moment-curvature relation by taking the nonlinear behavior of the materials into account. The moment-curvature relationships for different axial load level, transverse reinforcement diameter and transverse reinforcement spacing of the reinforced concrete column cross-sections were obtained considering Mander confined model. Moment-curvature relationships were obtained by SAP2000 Software which takes the nonlinear behavior of materials into consideration. The examined effects of the parameters on the column behavior were evaluated in terms of ductility and the strength of the cross-section. In the designed cross-sections, the effect of transverse reinforcement diameter and transverse reinforcement variation on the confined concrete strength and the moment-curvature relationship was calculated and compared for constant longitudinal reinforcement ratio. The examined behavioral effects of the parameters were evaluated by comparing the curvature ductility and the cross-section strength. It has been found that transverse reinforcement diameters and transverse reinforcement spacing are effective parameters on the ductility capacities of the column sections. Axial load is a very important parameter affecting the ductility of the section. It has been observed that the cross-sectional ductility of the column sections increases with the decrease in axial load.

***Keywords:*** *Transverse Reinforcement, Nonlinear, Confined Concrete Strength, Axial Load, Moment-Curvature, Curvature Ductility.*

## 1. INTRODUCTION

Understanding the nonlinear response and damage characteristics of reinforced concrete buildings subjected to significant earthquakes is essential for assessment of seismic performance of existing buildings, as well as safe and economic design of new buildings (Ucar *et al.*, 2015). In the reinforced concrete structures, that is known reinforced concrete columns are one of the most crucial elements under earthquake loads. Column mechanisms are very critical to prevent total collapse in earthquakes. The objective performance levels of reinforced concrete structures could not be ensured due to the failure of some critical reinforced concrete columns. Because of this, determining the behavior of the structures should be known well to design earthquake-resisting structures. In the reinforced concrete structures, the structural behavior can be changed according to the behavior of the reinforced concrete members. Moment-curvature relationship is one of the best solutions to evaluate and represent the behavior of reinforced concrete cross sections (Dok *et al.*, 2017).

The moment-curvature relationships of critical cross-sections of reinforced concrete members are essential for non-linear analysis of reinforced concrete structures. Realistic moment-curvature relationships can only be obtained if realistic material constitutive models are utilized for confined and unconfined concrete, and reinforcing steel during the cross-sectional moment-curvature analysis (Bedirhanoglu and Ilki, 2004). The behavior of reinforced concrete elements are determined by the cross-sectional behavior of elements. Cross-sectional behavior depends on the material used, the geometry of the cross-section and the loading on that particular cross-section. The behavior of a reinforced concrete cross-section under bending moment or bending moment plus axial force can be monitored from moment-curvature relationship (Ersoy and Özcebe, 2012). Moment-curvature relationship and stress-strain curves of steel and concrete are calculated by selecting Mander model (Mander et. al., 1988) and using the equilibrium equations and conformity equations to be written. Generally, the ductility is defined as the capacity of a material, section, structural element, or structure to undergo an excessive plastic deformation without a great loss in its load-carrying capacity (Arslan and Cihanli, 2010).

Ductility of reinforced structures is a desirable property where resistance to brittle failure during flexure is required to ensure structural integrity. Ductile behavior in a structure can be achieved through the use of plastic hinges positioned at appropriate locations throughout the structural frame. These are designed to provide sufficient ductility to resist structural collapse after the yield strength of the material has been achieved. The available ductility of plastic hinges in reinforced concrete is determined based on the shape of the moment-curvature relations (Olivia and Mandal, 2005). Ductility may be defined as the ability to undergo deformations without a substantial reduction in the flexural capacity of the member (Park and Ruitong, 1988). According to Xie et al, (1994), this deformability is influenced by some factors such as the tensile reinforcement ratio, the amount of longitudinal compressive reinforcement, the amount of lateral tie and the strength of concrete. The ductility of reinforced concrete section could be expressed in the form of the curvature ductility ($\mu_{\emptyset}$):

$$\mu_{\emptyset} = \emptyset_u/\emptyset_y \tag{1}$$

where $\emptyset_u$ ; is the curvature at ultimate when the concrete compression strain reaches a specified limiting value, $\emptyset_y$ ; is the curvature when the tension reinforcement first reaches the yield strength. Theoretical moment-curvature analysis for reinforced concrete structural elements indicating the available flexural strength and ductility can be constructed providing that the stress-strain relations for both concrete and steel are known. Moment-curvature relationship can be obtained from curvature and the bending moment of the section for a given load increased to failure (Olivia and Mandal, 2005).

In order to be able to understand the behavior of reinforced concrete members, cross sectional behavior should be known. Cross sectional behavior can be best evaluated by moment-curvature relationship. On a reinforced concrete cross section moment-curvature relationship can be determined by some complicated iteration methods. Making these iterations manually is very difficult and not practical. Some spread sheet programs can be used for this purpose (Çağlar *et al.*, 2013). Usually it is desirable to design a reinforced concrete member with sufficient curvature ductility capacity to avoid brittle failure in flexure and to insure a ductile behavior, especially under seismic conditions. Firstly, information about stress-strain relationships, confined concrete and unconfined concrete models, moment-curvature relationship is given for a better understanding of non-linear behavior (Foroughi and Yüksel, 2018).

In this study, squared reinforced concrete column cross section models with equal cross-sectional area were designed and the effect of the longitudinal reinforcement ratio, axial force level and transverse reinforcement ratio on the behavior of these models were investigated. The behavior of the column models was investigated through the relation of moment-curvature. In last decades various stress-strain relationships for unconfined and confined concrete were proposed by different researchers. A concrete model proposed by Mander *et al.* (1988) which is widely used, universally accepted and mandated in Turkish Seismic Code (TSC, 2018) has been used to determine the moment-curvature relationships of reinforced concrete members based on the SAP2000 Software (CSI, Ver. 20.1.0). Moment-curvature relations were obtained and presented in graphical form using SAP2000 Software which takes nonlinear behavior of materials into consideration. The examined behavioral effects of the parameters were evaluated by the curvature ductility and the cross-section strength. The stress-strain curves and moment-curvature curves were drawn in various models and were interpreted by comparing the curves.

## 2. MATERIAL AND METHOD

In order to investigate the effect of longitudinal reinforcement ratio and transverse reinforcement ratio, column models with dimensions of 400mm×400mm were designed. A total of 14 models were designed for different transverse reinforcement diameters, transverse reinforcement spacing and different axial loads of each model. The parameters investigated in the stress-strain relationships, confined concrete models, moment-curvature relations and ductility of the reinforced concrete column models are the transverse reinforcement diameter, transverse reinforcement spacing and axial load levels. The designed reinforced concrete cross section models are considered to be composed of three components; cover concrete, confined concrete and reinforcement steel. Material models are defined considering the Mander unconfined concrete model, for cover concrete, and the Mander confined concrete model for core concrete. For all column models, C30 was chosen as concrete grade and S420 was selected as reinforcement for the reinforcement behavior model, the stress-strain curves given in TSC (2018) were used (Table 1).

Table 1. Material parameters in property values (TS-500, 2000)

| Standard Strength | Parameters | Value |
|---|---|---|
| Concrete: C30 | Strain at maximum Stress of Unconfined Concrete ($\varepsilon_{co}$) | 0.002 |
| | Ultimate Compression Strain of Concrete ($\varepsilon_{cu}$) | 0.0035 |
| | Characteristic Standard Value of Concrete Compressive Strength ($f_{ck}$) | 30MPa |
| Reinforcement: S420 | Yield Strain of Reinforcement ($\varepsilon_{sy}$) | 0.0021 |
| | Spalling strain in reinforcing steel ($\varepsilon_{sp}$) | 0.008 |
| | Strain in reinforcing steel at maximum strength ($\varepsilon_{su}$) | 0.08 |
| | Characteristic Yield strength of Reinforcement ($f_{yk}$) | 420MPa |
| | Ultimate strength of Reinforcement ($f_{su}$) | 550MPa |

The details of the cross-sections with different transverse reinforcement diameters and transverse reinforcement spacing for different cross-sections are given in Table 2. As shown in Table 2, for the parametric study; transverse reinforcement spacing were taken as 50mm, 75mm, 100mm, 125mm, 150mm, 175mm and 200mm. Diameters of the transverse reinforcement diameters were taken as 8mm and 10mm.

Table 2. Details for the designed square column model cross-sections

| No | Longitudinal Reinforcement | Transverse reinforcement | $N/N_{max}$ |
|---|---|---|---|
| C1 | 8Φ22 | Φ8/50mm | 0<br>0.10<br>0.20<br>0.30<br>0.40 |
| C2 | | Φ8/75mm | |
| C3 | | Φ8/100mm | |
| C4 | | Φ8/125mm | |
| C5 | | Φ8/150mm | |
| C6 | | Φ8/175mm | |
| C7 | | Φ8/200mm | |
| C8 | 8Φ22 | Φ10/50mm | 0<br>0.10<br>0.20<br>0.30<br>0.40 |
| C9 | | Φ10/75mm | |
| C10 | | Φ10/100mm | |
| C11 | | Φ10/125mm | |
| C12 | | Φ10/150mm | |
| C13 | | Φ10/175mm | |
| C14 | | Φ10/200mm | |

The combined effect of $N_{dmax}$ vertical loads and seismic loads, gross section area of column shall satisfy the condition $A_c \geq N_{dmax}/0.40f_{ck}$, (TSC, 2018). To investigate the effect of axial force on the cross-section behavior, the models were investigated under five different axial forces; $N_1 = 0$, $N_2$=480kN, $N_3$=960kN, $N_4$ =1440kN and $N_5$ =1920kN. Moment-curvature relationships for the designed column cross-sections are presented from the analytical results of different axial load, transverse reinforcement diameter and transverse reinforcement spacing. By using the Mander model, with the consideration of the lateral confining stress, the σ-ε relationships of the reinforced concrete columns are obtained by using the SAP2000 Software. The reinforcement diameters and reinforcement ratio used in the cross-sections were determined by considering the limitations given TS500 (2000) and TSC (2018). In all the models the longitudinal column reinforcement was 8Φ22. The monotonic envelope curve introduced by Mander *et al.* (1988) was adopted in this study for its computational efficiency. The following equation is used to calculate the unconfined concrete strength ( $f'_{cc}$ ). The effectively confined area of concrete at hoop level is found by subtracting the area of the parabolas containing the ineffectively confined concrete. Thus the total plan area of ineffectually confined core concrete at the level of the hoops when there are n longitudinal bars is;

$$A_i = \frac{\sum_i^n (w_i')^2}{6} \tag{1}$$

Incorporating the influence of the ineffective areas in the elevation, the area of effectively confined concrete core at midway between the levels of transverse hoop reinforcement is:

$$A_e = \left(b_c\, d_c - \sum_i^n \frac{(w_i')^2}{6}\right)\left(1 - \frac{S'}{2b_c}\right)\left(1 - \frac{S'}{2d_c}\right) \tag{2}$$

Where $b_c$; concrete core dimension to center line of perimeter hoop in x-direction, $d_c$ ; concrete core dimension to center line of perimeter hoop in y direction, $s'$; clear vertical spacing between hoops. Therefore, the confinement effectiveness coefficient $(k_e)$ , which represents the ratio of the smallest effectively confined concrete area $(A_e)$ to the net confined concrete core area $(A_{cc})$, could be given by the following Equations.

$$k_e = \frac{A_e}{A_{cc}} \quad , \quad A_{cc} = b_c\, d_c(1 - \rho_{cc}) \tag{3}$$

$\rho_{cc}$ is ratio of area of longitudinal reinforcement to area of concrete core.

It is possible for rectangular reinforced concrete members to have different quantities of transverse confining steel in the x and y directions. These may be expressed as,

$$\rho_s = \rho_x + \rho_y = \frac{A_{sx}}{s\, d_c} + \frac{A_{sy}}{s\, b_c} \tag{4}$$

The lateral confining stress on the concrete (total transverse bar force divided by vertical area of confined concrete) are given in the x and y direction as,

$$f_{lx} = \rho_x\, f_{yh} \quad , \quad f_{ly} = \rho_y\, f_{yh} \tag{5}$$

Effective lateral confining stresses in the x and y directions are,

$$f'_{lx} = k_e\, f_{lx} \quad , \quad f'_{ly} = k_e\, f_{ly} \quad , \quad f'_l = f_l\, k_e \tag{6}$$

To determine the confined concrete compressive strength $f'_{cc}$, a constitutive model involving a specified maximum strength surface for multiaxial compressive stresses is used in this model. $f'_l$ is the effective lateral confining stress.

$$f'_{cc} = f'_{co}\left(-1.254 + 2.254\sqrt{\frac{1 + 7.94 f'_l}{f'_{co}}} - 2\frac{f'_l}{f'_{co}}\right) \tag{7}$$

The longitudinal concrete stress ($f_c$) is given by the following relation as the function of the longitudinal concrete strain ($\varepsilon_c$). In the following equations, $f_c$ and $\varepsilon_c$ represent the concrete strength and the corresponding strain value, respectively.

$$f_c = \frac{f'_{cc}\, x\, r}{r - 1 + x^r} \quad , \quad x = \frac{\varepsilon_c}{\varepsilon_{cc}} \tag{8}$$

Where $\varepsilon_c$: longitudinal compressive concrete strain. The calculation of $f'_{cc}$ is not sufficient to obtain stress-strain curve of confined concrete. Therefore, the corresponding strain at maximum concrete stress ($\varepsilon_{cc}$) has to be calculated too. In addition, the maximum unit strain value '$\varepsilon_{cu}$' in the concrete must be calculated at the first hoop fracture occurring in transverse reinforcement.

$$\varepsilon_{cc} = \varepsilon_{co}\left[1 + 5\left(\frac{f'_{cc}}{f'_{co}} - 1\right)\right] \tag{9}$$

Where $f'_{co}$ and $\varepsilon_{co}$; the unconfined concrete strength and corresponding strain, respectively (generally $\varepsilon_{co} = 0.002$ can be assumed), and

$$r = \frac{E_c}{E_c - E_{sec}} \tag{10}$$

$$E_c = 5000\sqrt{f'_{co}}\; MPa \, , \quad E_{sec} = \frac{f'_{cc}}{\varepsilon_{cc}} \tag{11}$$

$E_c$: modulus of elasticity of concrete
$E_{sec}$: secant modulus of confined concrete at peak stress

Maximum concrete compressive strain (fracture strain $\varepsilon_{cu}$) is defined as the fracturing of the confining reinforcement. Maximum concrete compressive strain for confined concrete is given (Paulay and Priestley, 1992);

$$\varepsilon_{cu} = 0.004 + \frac{1.4\, \rho_s\, f_{yw}\, \varepsilon_{su}}{f'_{cc}} \tag{12}$$

$\rho_s$: ratio of volume to transverse confining steel to volume of confined concrete core
$\varepsilon_{su}$: Strain in reinforcing steel at maximum strength
$f_{yw}$: yield strength of transverse reinforcement

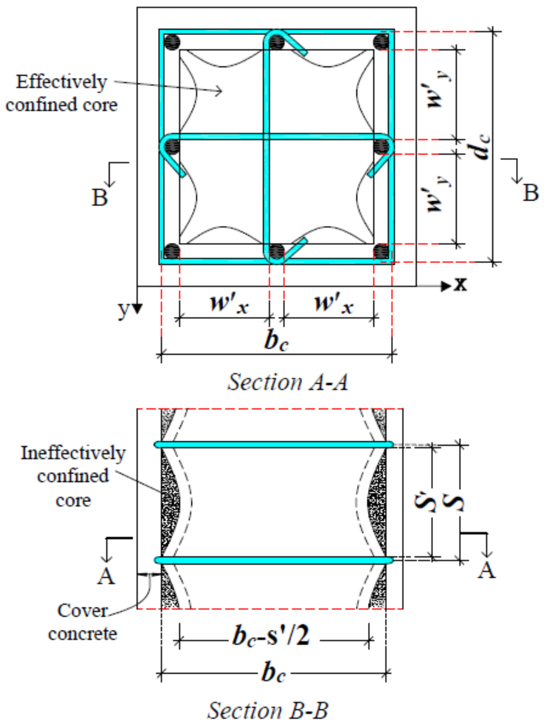


Fig. 1. Effectively confined core for square hoop reinforcement (Mander *et al.*, 1988)

## 3. NUMERICAL STUDY

The computed results for the models are summarized in the following Tables. When the calculated values of the designed models were examined, the following results were obtained. The values given in the tables are prepared according to the different confining reinforcement diameters and spacing for the column models. Effective lateral confining stress in *x* and *y* direction and compressive strength of confined concrete and $\varepsilon_{cc}$ and $\varepsilon_{cu}$ values are given in Table 3. The obtained σ-ε relationship of the longitudinal concrete stress ($f_c$) as the function of the longitudinal concrete strain ($\varepsilon_c$) is summarized in Fig. 2. The σ-ε curve shown in Fig. 1 for different transverse reinforcement spacing has been prepared according to 8mm (Fig. 2a) and 10 mm (Fig. 2b) transverse reinforcement diameter.

Table 3. The calculated $f_{lx}$, $f_{ly}$, $f'_{lx}$, $f'_{ly}$, $f'_l$, $f'_{cc}$, $\varepsilon_{cc}$ and $\varepsilon_{cu}$ values to Mander models

| No | Hoops spacing(mm) | $f_{lx}, f_{ly}$ (MPa) | $f'_{lx}, f'_{ly}, f'_l$ (MPa) | $f'_{cc}$ (MPa) | $\varepsilon_{cc}$ | $\varepsilon_{cu}$ |
|---|---|---|---|---|---|---|
| C1 | Φ8/50 | 3.838 | 2.767 | 40.91 | 0.0080 | 0.0302 |
| C2 | Φ8/75 | 2.558 | 1.698 | 35.69 | 0.0059 | 0.0240 |
| C3 | Φ8/100 | 1.919 | 1.168 | 32.81 | 0.0048 | 0.0203 |
| C4 | Φ8/125 | 1.535 | 0.845 | 30.98 | 0.0041 | 0.0178 |
| C5 | Φ8/150 | 1.279 | 0.648 | 29.73 | 0.0036 | 0.0160 |
| C6 | Φ8/175 | 1.096 | 0.503 | 28.83 | 0.0033 | 0.0146 |
| C7 | Φ8/200 | 0.959 | 0.396 | 28.15 | 0.0030 | 0.0135 |
| C8 | Φ10/50 | 5.961 | 4.341 | 47.48 | 0.0106 | 0.0391 |
| C9 | Φ10/75 | 3.974 | 2.666 | 40.45 | 0.0078 | 0.0315 |
| C10 | Φ10/100 | 2.980 | 1.836 | 36.41 | 0.0062 | 0.0269 |
| C11 | Φ10/125 | 2.384 | 1.344 | 33.79 | 0.0052 | 0.0237 |
| C12 | Φ10/150 | 1.987 | 1.020 | 31.96 | 0.0045 | 0.0214 |
| C13 | Φ10/175 | 1.703 | 0.793 | 30.62 | 0.0040 | 0.0195 |
| C14 | Φ10/200 | 1.490 | 0.626 | 29.60 | 0.0036 | 0.0180 |

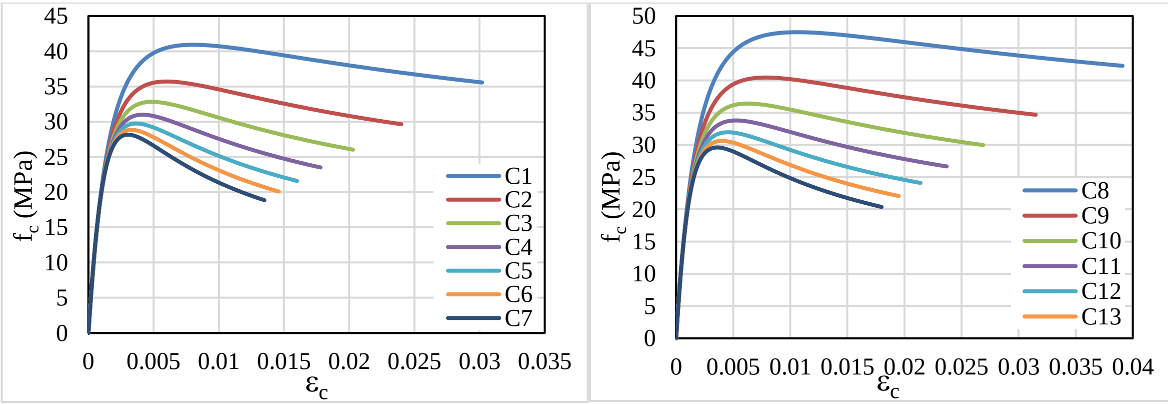


(a) (b)

Fig. 2. Stress-strain relationships for different transverse reinforcement spacing according to Mander model

The moment-curvature relationships obtained from the analytical results are presented in graphical form. Fig. 3 shows the moment-curvature comparisons for different transverse reinforcement spacing and different axial loads in the designed cross sections. In Fig. 3, moment-curvature relationships are given for different transverse reinforcement spacings according to the transverse reinforcement diameters of 8mm and 10mm respectively. In the column models designed from the analytical results, while the axial load is fixed in Fig. 4, the moment-curvature relationships are compared with respect to the diameter and spacing of different transverse reinforcements.

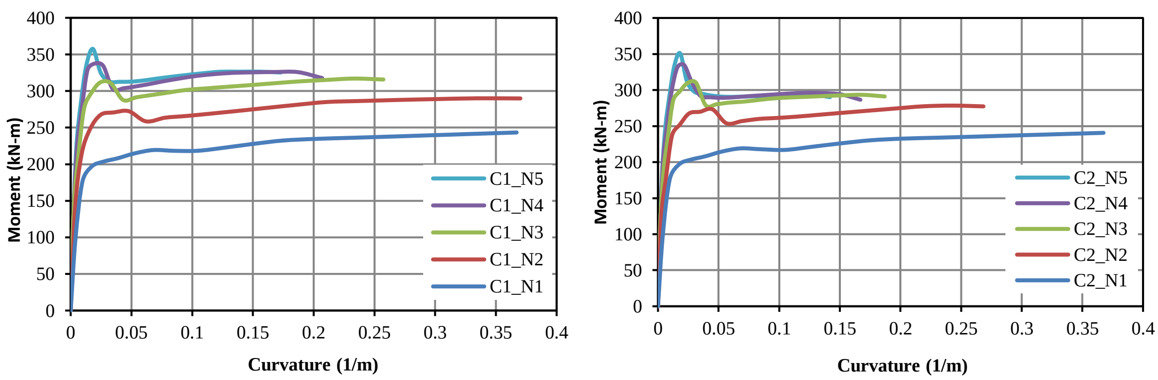

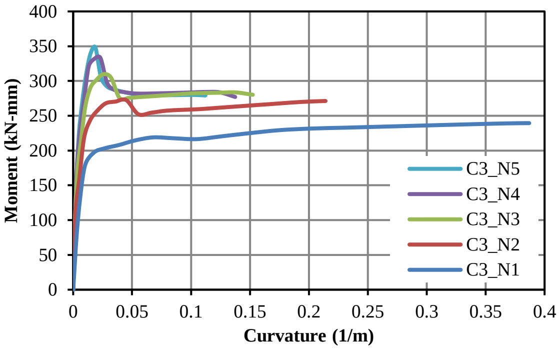
Moment (kN-mm)
Curvature (1/m)
C3_N5
C3_N4
C3_N3
C3_N2
C3_N1

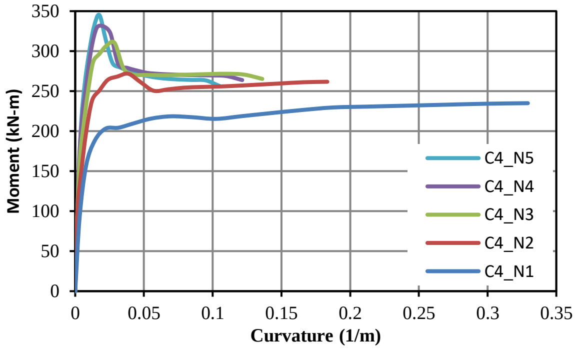
Moment (kN-m)
Curvature (1/m)
C4_N5
C4_N4
C4_N3
C4_N2
C4_N1

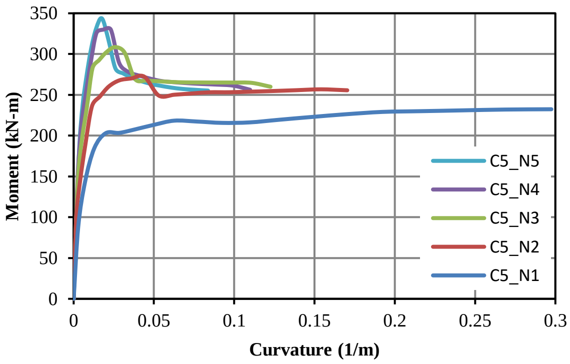
Moment (kN-m)
Curvature (1/m)
C5_N5
C5_N4
C5_N3
C5_N2
C5_N1

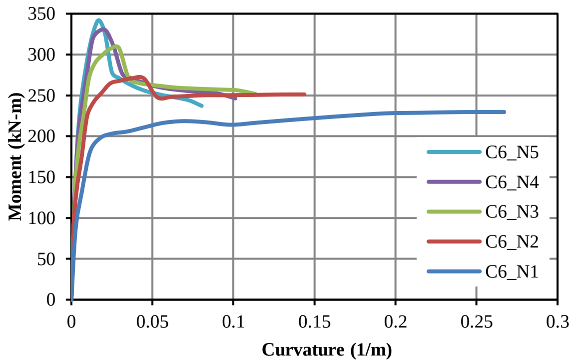
Moment (kN-m)
Curvature (1/m)
C6_N5
C6_N4
C6_N3
C6_N2
C6_N1

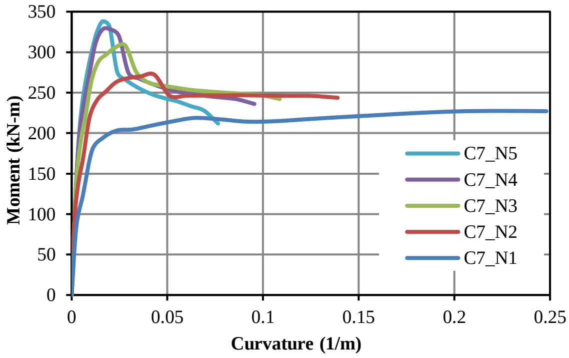
Moment (kN-m)
Curvature (1/m)
C7_N5
C7_N4
C7_N3
C7_N2
C7_N1

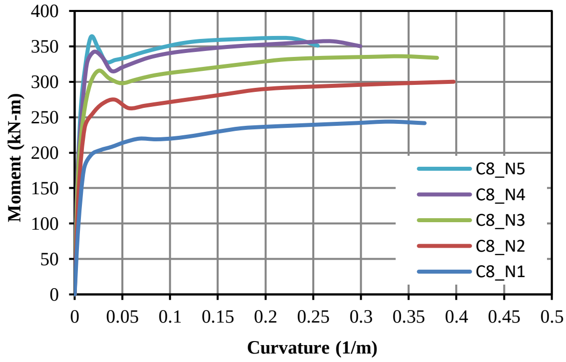
Moment (kN-m)
Curvature (1/m)
C8_N5
C8_N4
C8_N3
C8_N2
C8_N1

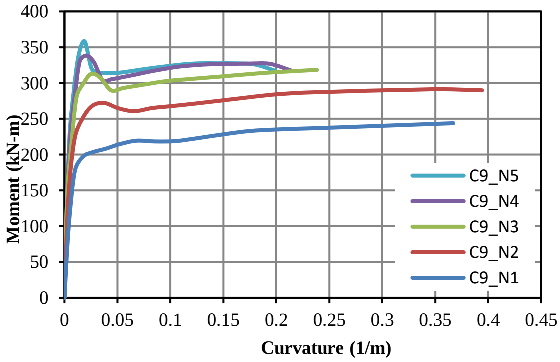
Moment (kN-m)
Curvature (1/m)
C9_N5
C9_N4
C9_N3
C9_N2
C9_N1

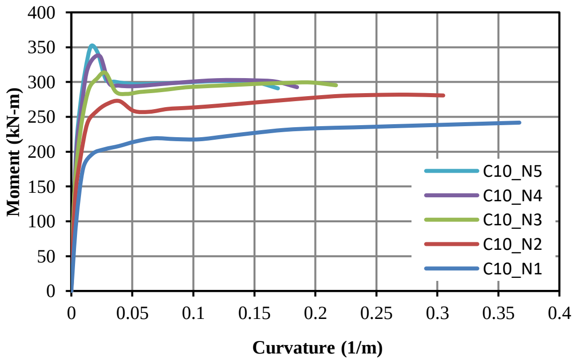
Moment (kN-m)
Curvature (1/m)
C10_N5
C10_N4
C10_N3
C10_N2
C10_N1

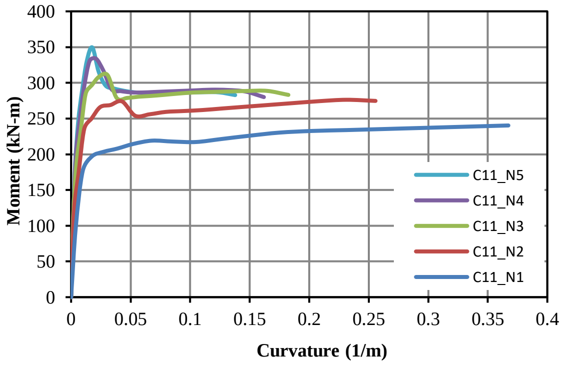
Moment (kN-m)
Curvature (1/m)
C11_N5
C11_N4
C11_N3
C11_N2
C11_N1

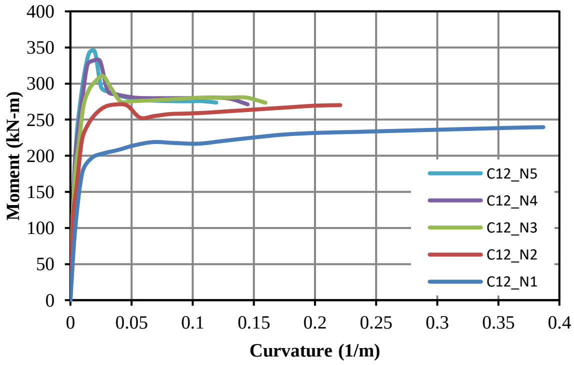
Moment (kN-m)
Curvature (1/m)
C12_N5
C12_N4
C12_N3
C12_N2
C12_N1

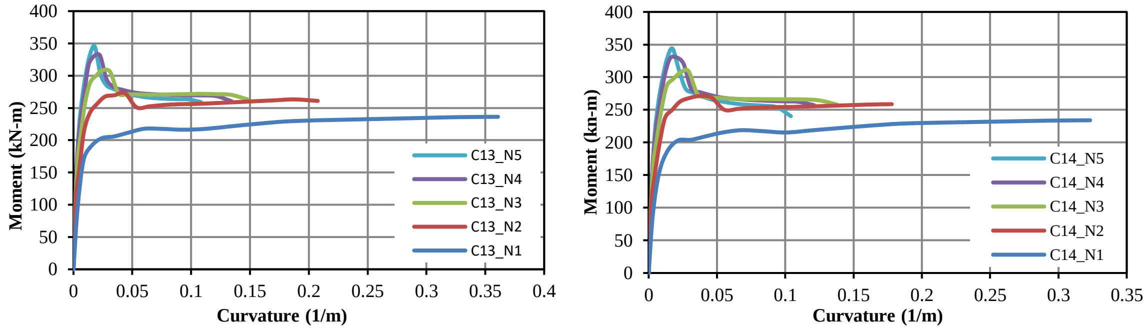


Fig. 3. Moment-curvature relationships of the columns for different load axial

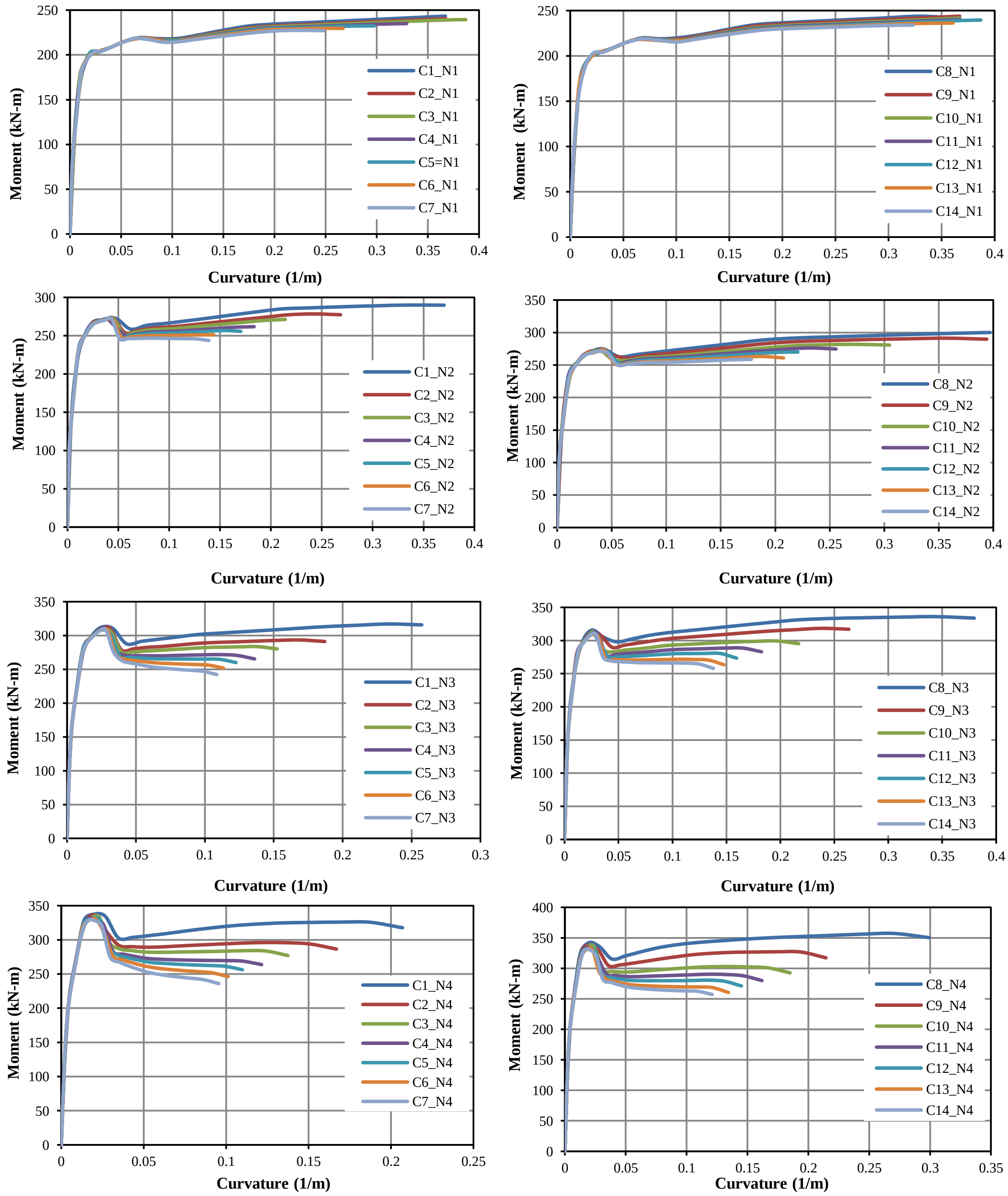

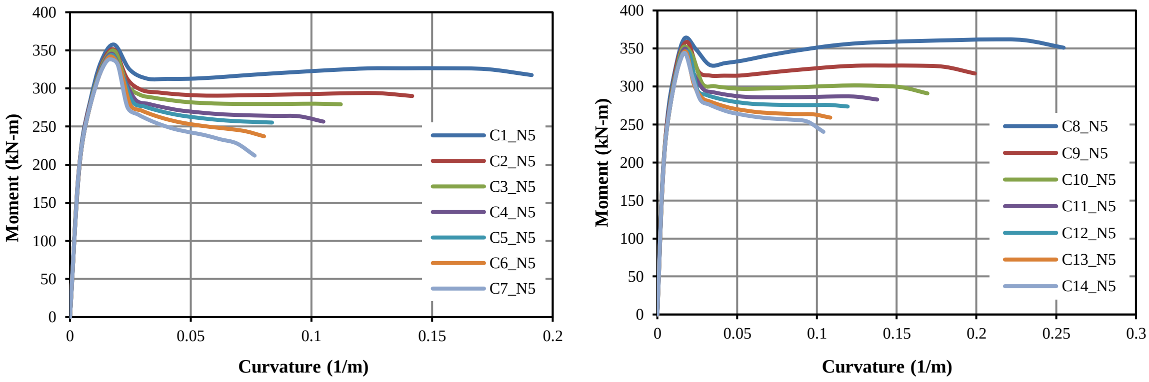


Fig. 4. Moment-curvature relationships of the columns for different hoops spacing

Moment-curvature relationships for the designed column cross-sections are presented for different axial load level, transverse reinforcement diameter and transverse reinforcement spacing. Yield moment ($\boldsymbol{M_y}$), ultimate moment ($\boldsymbol{M_u}$), yield curvatures ($\emptyset_y$), ultimate curvatures ($\boldsymbol{\emptyset_u}$) and curvature ductility ($\boldsymbol{\mu_\emptyset}$) values are calculated from the moment-curvature relationships (Table 4 and Table 5).

Table 4. Calculation results of bending moment-curvature (transverse reinforcement Φ8)

| Kesit No | Axial Load Level $N/N_{max}$ | $M_y$ $(kN.m)$ | $\emptyset_y$ $(1/m)$ | $M_u$ $(kN.m)$ | $\emptyset_u$ $(1/m)$ | $\mu_\emptyset$ |
|---|---|---|---|---|---|---|
| C1 | 0 | 165.03 | 0.0088 | 243.32 | 0.4060 | 46.1 |
| | 0.1 | 218.78 | 0.0101 | 290.0 | 0.3258 | 32.3 |
| | 0.2 | 278.27 | 0.0116 | 317.0 | 0.2574 | 22.2 |
| | 0.3 | 322.15 | 0.0132 | 337.54 | 0.2070 | 15.7 |
| | 0.4 | 345.35 | 0.0153 | 357.52 | 0.1913 | 12.5 |
| C2 | 0 | 164.56 | 0.0088 | 240.58 | 0.4063 | 46.2 |
| | 0.1 | 220.07 | 0.0101 | 278.43 | 0.2688 | 26.6 |
| | 0.2 | 275.65 | 0.0116 | 291.10 | 0.1870 | 16.1 |
| | 0.3 | 312.53 | 0.0132 | 334.72 | 0.1669 | 12.6 |
| | 0.4 | 342.07 | 0.0157 | 350.88 | 0.1418 | 9.0 |
| C3 | 0 | 164.41 | 0.0088 | 239.42 | 0.4064 | 46.2 |
| | 0.1 | 222.45 | 0.0101 | 272.42 | 0.2141 | 21.2 |
| | 0.2 | 271.35 | 0.0116 | 309.77 | 0.1524 | 13.1 |
| | 0.3 | 321.69 | 0.0134 | 333.42 | 0.1375 | 10.3 |
| | 0.4 | 341.57 | 0.0159 | 348.16 | 0.1122 | 7.1 |
| C4 | 0 | 161.15 | 0.0087 | 234.96 | 0.3293 | 37.9 |
| | 0.1 | 218.33 | 0.0101 | 271.76 | 0.1834 | 18.2 |
| | 0.2 | 272.56 | 0.0116 | 310.29 | 0.1361 | 11.7 |
| | 0.3 | 313.68 | 0.0133 | 263.84 | 0.1215 | 9.1 |
| | 0.4 | 339.80 | 0.0161 | 345.20 | 0.1050 | 6.5 |
| C5 | 0 | 155.18 | 0.0087 | 232.37 | 0.2975 | 34.2 |
| | 0.1 | 221.70 | 0.0101 | 272.26 | 0.1704 | 16.9 |
| | 0.2 | 282.77 | 0.0117 | 308.54 | 0.1226 | 10.5 |
| | 0.3 | 318.12 | 0.0134 | 329.95 | 0.1099 | 8.2 |
| | 0.4 | 338.59 | 0.0161 | 343.63 | 0.0837 | 5.2 |
| C6 | 0 | 154.09 | 0.0087 | 229.66 | 0.2671 | 30.7 |
| | 0.1 | 226.30 | 0.0101 | 270.75 | 0.1438 | 14.2 |
| | 0.2 | 275.13 | 0.0116 | 308.07 | 0.1135 | 9.8 |
| | 0.3 | 319.52 | 0.0134 | 329.25 | 0.1012 | 7.6 |
| | 0.4 | 337.90 | 0.0159 | 341.98 | 0.0804 | 5.1 |
| C7 | 0 | 156.52 | 0.0087 | 227.42 | 0.2481 | 28.5 |
| | 0.1 | 223.78 | 0.0101 | 272.11 | 0.1390 | 13.8 |
| | 0.2 | 273.01 | 0.0116 | 308.02 | 0.1087 | 9.4 |
| | 0.3 | 315.11 | 0.0134 | 328.22 | 0.0955 | 7.1 |
| | 0.4 | 336.94 | 0.0158 | 338.0 | 0.0765 | 4.8 |

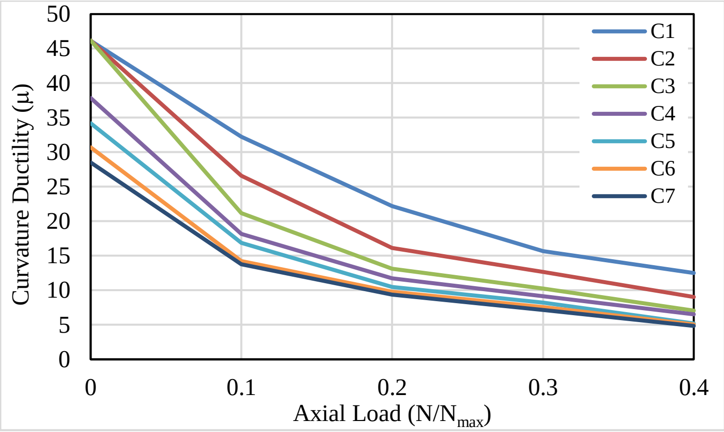


Fig. 5. Influence of axial loads on the ductility (transverse reinforcement Φ8).

Table 5. Calculation results of bending moment-curvature (transverse reinforcement Φ10)

| Kesit No | Axial Load Level $N/N_{max}$ | $M_y$ $(kN.m)$ | $\emptyset_y$ $(1/m)$ | $M_u$ $(kN.m)$ | $\emptyset_u$ $(1/m)$ | $\mu_\emptyset$ |
|---|---|---|---|---|---|---|
| C8 | 0 | 165.53 | 0.0089 | 243.81 | 0.4120 | 46.3 |
| | 0.1 | 232.02 | 0.0102 | 300.10 | 0.3671 | 36.0 |
| | 0.2 | 265.02 | 0.0114 | 336.07 | 0.3297 | 28.9 |
| | 0.3 | 326.50 | 0.0131 | 357.16 | 0.2994 | 22.9 |
| | 0.4 | 349.53 | 0.0151 | 351.02 | 0.2547 | 16.9 |
| C9 | 0 | 165.06 | 0.0088 | 243.85 | 0.4058 | 46.1 |
| | 0.1 | 223.98 | 0.0101 | 291.33 | 0.3423 | 33.9 |
| | 0.2 | 280.96 | 0.0116 | 318.39 | 0.2635 | 22.7 |
| | 0.3 | 318.20 | 0.0132 | 338.32 | 0.2145 | 16.3 |
| | 0.4 | 345.66 | 0.0153 | 358.20 | 0.1990 | 13.0 |
| C10 | 0 | 164.66 | 0.0088 | 241.70 | 0.4061 | 46.1 |
| | 0.1 | 213.57 | 0.010 | 281.82 | 0.3048 | 30.5 |
| | 0.2 | 268.11 | 0.0115 | 313.14 | 0.2169 | 18.9 |
| | 0.3 | 316.68 | 0.0133 | 336.15 | 0.185 | 13.9 |
| | 0.4 | 349.44 | 0.0159 | 351.59 | 0.1693 | 10.6 |
| C11 | 0 | 164.50 | 0.0088 | 240.29 | 0.4062 | 46.2 |
| | 0.1 | 224.67 | 0.0101 | 276.25 | 0.2557 | 25.3 |
| | 0.2 | 278.35 | 0.0117 | 310.92 | 0.1825 | 15.6 |
| | 0.3 | 312.89 | 0.0132 | 333.79 | 0.1619 | 12.3 |
| | 0.4 | 341.62 | 0.0158 | 349.44 | 0.1378 | 8.7 |
| C12 | 0 | 164.38 | 0.0088 | 239.58 | 0.4063 | 46.2 |
| | 0.1 | 224.88 | 0.0101 | 271.02 | 0.2208 | 21.9 |
| | 0.2 | 273.50 | 0.0116 | 310.35 | 0.1595 | 13.8 |
| | 0.3 | 320.98 | 0.0134 | 331.76 | 0.1450 | 10.8 |
| | 0.4 | 342.99 | 0.0161 | 344.22 | 0.1193 | 7.4 |
| C13 | 0 | 170.62 | 0.0088 | 236.27 | 0.3608 | 41.0 |
| | 0.1 | 220.34 | 0.0101 | 272.89 | 0.2076 | 20.6 |
| | 0.2 | 270.50 | 0.0116 | 308.37 | 0.1477 | 12.7 |
| | 0.3 | 318.40 | 0.0134 | 331.42 | 0.1344 | 10.0 |
| | 0.4 | 338.95 | 0.0161 | 345.02 | 0.1084 | 6.7 |
| C14 | 0 | 159.74 | 0.0087 | 234.02 | 0.3232 | 37.1 |
| | 0.1 | 219.22 | 0.0101 | 271.09 | 0.1780 | 17.6 |
| | 0.2 | 271.78 | 0.0116 | 309.52 | 0.1380 | 11.9 |
| | 0.3 | 313.48 | 0.0133 | 330.44 | 0.1210 | 9.1 |
| | 0.4 | 338.36 | 0.0160 | 343.85 | 0.1041 | 6.5 |

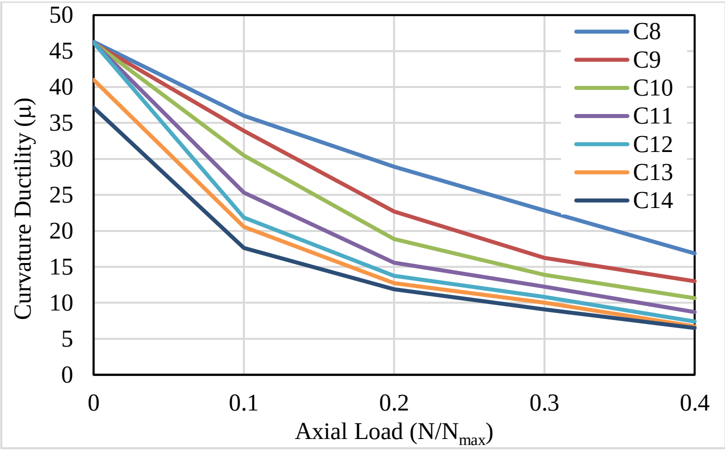


Fig. 6. Influence of axial loads on the ductility (transverse reinforcement Φ10).

In this part of the study, the moment-curvature diagrams are obtained from the SAP2000 Software by changing the transverse reinforcement diameter, transverse reinforcement spacing and axial load level. When the analysis results are examined, it is observed that the variation of the axial load and transverse reinforcement have important effect on the moment-curvature behavior of the reinforced concrete cross-sections. As a result, axial load is a very important parameter affecting the ductility of the section. As it shall be seen from moment-curvature relations, ductility decreases with the increase of axial load ($N/N_{max} \geq 0$) ratio where the transverse reinforcement is constant. However, when the axial load is small in the same cross-sections (transverse reinforcement is constant), the ductility in the cross-section is high. As it can be seen from the moment-curvature graphs, it is observed that the cross-section ductility decreases when the transverse reinforcement spacing is increased under a constant axial load. It is observed that the cross-section ductility and the curvature increase significantly with the reduction of the transverse reinforcement spacing. It is observed that the ratio of transverse reinforcement is effective on cross-section behavior of reinforced concrete cross section. The increase in transverse reinforcement diameter increases the ductility of the cross section and the maximum moment bearing capacity.

## 4. CONCLUSION

The following results were obtained from the stress-strain and moment-curvature analyses of the square columns:

The stress-strain relationship graphs of confined compressive strength and corresponding axial strain, of the core regions of the reinforced concrete columns are investigated based on the numerical study. The following results were obtained from the comparison of the columns with different characteristics of the examined factor in the study. The models were examined according to the conditions given in the TSC, (2018). Concrete stress-strain graphs were obtained by using Mander confined concrete models. Although the longitudinal reinforcement diameters and reinforcement yield strengths used in the models are constant, the effect of the use of different transverse reinforcement diameters and transverse reinforcement spacing on the lateral effective strength was investigated.

- It has been found that for all models, transverse reinforcement diameters and transverse reinforcement spacing are effective on the lateral load bearing capacity.
- The transverse reinforcement spacing densification has a greater effect on the ductility and the bearing capacity (moment capacity) of a cross section.
- The increase of the transverse reinforcement ratio increases the ductility and the maximum bearing capacity of a cross section.
- The moment-curvature relationship is determined according to the cross-sectional analysis of reinforced concrete columns by using SAP2000. The moment-curvature relationships are compared according to transverse reinforcement diameters, transverse reinforcing spacing and the axial load levels of reinforced concrete columns.
- The result is that the axial load is a very important parameter affecting the ductility of the cross-section. The relationship between axial load and ductile behavior is generally inversely proportional (Figs. 3 and 4).
- The increase in the axial load level causes the curvature values to decrease (brittle behavior), although it usually increases the moment capacity of the cross section.
- It has been observed that the cross-sectional ductility increases with the decrease in axial load.
- In cases where the axial load is small, reinforced concrete sections have a ductile behavior.
- As the diameter of the transverse reinforcement increases, the moment capacity of the cross section increases as expected.
- Significant reductions in ductility capacities under increasing axial force have been observed.
- The effect of axial load on cross-sectional behavior appears to be more explicit in cross sections where the transverse reinforcement spacing is minimum.
- If the analysis results are compared, yielding and ultimate moment capacities of the sections increase when decrease of the transverse reinforcement spacing.
- Moreover, the more ductile behavior for reinforced concrete cross sections is observed due to

increment of curvature ductility on reinforced concrete square columns with the increase of transverse reinforcing ratio.

- Additionally, according to the analysis results, the increment of transverse reinforcement ratio affects the yielding and ultimate moment capacities of the members for each type of concrete material.
- In order to see the actual behavior of the column sections, the transverse reinforcement ratio, transverse reinforcement spacing, and axial load ratio should be taken into consideration in the analyses.

## REFERENCES

Arslan, G. and Cihanli, E. (2010). "Curvature Ductility Prediction of Reinforced High-Strength Concrete Beam Sections." *Journal of Civil Engineering and Management*, Vol. 16, No. 4, pp. 462–470.

Bedirhanoglu, I. And Ilki, A. (2004). "Theoretical Moment-Curvature Relationships for Reinforced Concrete Members and Comparison with Experimental Data." *Sixth International Congress on Advances in Civil Engineering*, 6-8 October 2004 Bogazici University, Istanbul, Turkey, pp. 231-240.

Caglar, N., Ozturk, H., Demir, A., Akkaya, A. and Pala, M. (2013). "Betonarme Kesitlerdeki Moment-Eğrilik İlişkisinin Yapay Sinir Ağları ile Belirlenmesi." *Akademik Platform Mühendislik ve Fen Bilimleri Dergisi*, pp. 1018-1029.

Ersoy, U. ve Özcebe, G. (2012). *Betonarme 1*, Evrim Yayınevi ve Bilgisayar San. TİC. LTD. ŞTİ. İstanbul, Türkiye.

Dok, G., Ozturk, H. and Demir, A. (2017). "Determining Moment-Curvature Relationship of Reinforced Concrete Columns." *The Eurasia Proceedings of Science, Technology, Engineering and Mathematics*, (EPSTEM), Vol. 1, pp. 52-58.

Foroughi, S. and Yuksel, S.B. (2018). "Moment Curvature Relationship of Square Columns." *International Congress on Engineering and Architecture*, (ENAR), Alanya, Turkey, pp. 681-688.

Olivia, M. and Mandal, P. (2005). "Curvature Ductility Factor of Rectangular Sections Reinforced Concrete Beams." *Journal of Civil Engineering*, Vol. 16, No. 1, pp. 1-13.

Mander, J. B., Priestley, M. J. N. and Park, R. (1988). "Theoretical stress-strain model for confined concrete." *Journal of Structural Engineering*, Vol. 114, No. 8, pp. 1804-1826.

Paulay, T., and Priestley, M.J.N. (1992). *Seismic Design of Reinforced Concrete and Masonry Buildings*, John Wiley & Sons, Inc, New York, USA.

Park, R. and Ruitong, D. (1988). "Ductility of doubly reinforced concrete beam section." *ACI Structural Journal*, Vol. 85, No. 2, pp. 217-225.

SAP2000, Structural Software for Analysis and Design, Computers and Structures, Inc, USA.

TSC (2018). *Specification for Buildings to be Built in Seismic Zones*, Ministry of Public Works and Settlement Government of the Republic of Turkey.

TS500 (2000). *Requirements for Design and Construction of Reinforced Concrete Structures*, Turkish Standards Institute, Ankara, Turkey.

Ucar, T., Merter, O. and Duzgun, M., (2015). "Determination of lateral strength and ductility characteristics of existing mid-rise RC buildings in Turkey." *Computers and Concrete*, Vol. 16, No. 3, pp. 467-485.

Xie, Y., Ahmad, S., Yu, T., Hino, S. and Chung, W. (1994). "Shear ductility of reinforced concrete beams of normal and high strength concrete." *ACI Structural Journal*, Vol. 91, No. 2, pp. 140-149.